Applied Catalysis B: Environmental 123–124 (2012) 43–51

Contents lists available at SciVerse ScienceDirect

Applied Catalysis B: Environmental

journal homepage: www.elsevier.com/locate/apcatb

Photodegradation of phenanthrene on cation-modified clays under visible light

Hanzhong Jia [a], Jincai Zhao [b], Xiaoyun Fan [a], Kamila Dilimulati [a], Chuanyi Wang [a,*]

[a] Laboratory of Eco-Materials and Sustainable Technology (LEMST), Xinjiang Technical Institute of Physics & Chemistry, Chinese Academy of Sciences, Urumqi, Xinjiang 830011, China
[b] Key Laboratory of Photochemistry, Institute of Chemistry, Chinese Academy of Sciences, Beijing 100190, China

ARTICLE INFO

Article history:
Received 17 January 2012
Received in revised form 11 April 2012
Accepted 14 April 2012
Available online 21 April 2012

Keywords:
Polycyclic aromatic hydrocarbons (PAHs)
Phenanthrene
Clay minerals
Visible light photodegradation
Fenton-like reaction

ABSTRACT

Transformation and fate of polycyclic aromatic hydrocarbons (PAHs) are critically influenced by natural conditions, especially their interactions with various components of soils and sediments. In the present study, phenanthrene was employed as a model to explore the potential photocatalysis effect of various cation-modified clay minerals in the soil under visible-light irradiation. For five types of cation-modified smectite clays, the photodegradation rates of phenanthrene follow the order: $Fe^{3+} > Cu^{2+} > > Ca^{2+} > K^{+} > Na^{+}$, which is explained in terms of photo-Fenton-like catalysis. To further inspect the effect of clay type, additional two types of clays were paralleled. Among three types of Fe(III)-modified clays, Fe(III)-smectite shows the highest photodegradation rate followed by Fe(III)-vermiculite and Fe(III)-kaolinite. The photoactivity order is consistent with the iron content contained in the three clays, suggesting that Fe(III) content plays an important role in photocatalytic degradation of phenanthrene. The reactivity of iron species greatly depends on the interlayer microenvironment of smectite such as pH and water content. Moreover, phthalates, 9,10-phenanthrenequinone and alkanoic acids were identified by GC/MS analyses as the main intermediate compounds, and the organic compounds were mineralized finally. The overall results provide valuable insights on the transformation and fate of PAHs in the natural soil environment.

1. Introduction

Polycyclic aromatic hydrocarbons (PAHs), mainly produced via fossil fuel deposit and incomplete combustion, have been ubiquitously found in natural phases such as water, soil, and sediment. Due to their persistence to natural degradation and potential damaging to human health and ecosystem, PAHs have been classified as priority pollutants by the US Environmental Protection Agency (USEPA water quality criteria) [1–3]. Phenanthrene is one of the most widespread PAHs with three fused benzene rings, and it is often used as a model compound to study the fate of PAHs in contaminated soils [4,5].

The photolysis of PAHs is a potentially important process for its stability and fate in the soil environment [6]. Under natural sunlight or UV light, PAHs that can be removed from soil include pyrene, benzo[*a*]pyrene, and phenanthrene [7–10]. Photolysis occurs within a shallow depth, highly depending on the soil characteristics, such as particle size, pH value, and humidity [7,11–13]. The soil components, such as metal oxide, humic acid, natural minerals, also significantly impact the photolysis. Photochemical behavior of benzo[*a*]pyrene on soil surface under UV light irradiation can be enhanced by the addition of Fe_2O_3 and TiO_2 in the reaction system [9]. The MnO_2-oxidative degradation of pyrene was significantly enhanced in the presence of alluvial and red soils [14]. Co-existence of humic acid and dodecylbenzenesulfonate could accelerate the photodegradation rate of PAHs [13]. Iron oxides and oxalic acid can generate a photo-Fenton-like system without H_2O_2 addition in solid phase to enhance the photodegradation of pyrene under UV irradiation [8]. In addition, the photolysis rate of pesticides such as atrazine follows the order of clay > silt > sand, suggesting that clay in soil might favor the photochemical reaction [12,13].

Clay minerals are generally considered as one class of the most chemically active components of soils. They may strongly influence the fate of environmental contaminants in soils, subsoils, aquifers, and sediments. Various clay minerals have shown great capability of adsorbing PAHs, suggesting the potential importance of clays in soils and subsoils [5,15,16]. However, limited work has been done to probe the photochemical behavior of PAHs on clay minerals, and the role regulated by the clay structural and physicochemical properties is also poorly understood. Those properties, such as clay type, surface charge density, cation exchange capacity, and exchangeable cations, are critical to understanding the fate of contaminants in the soil environment. Among soil minerals, 2:1 aluminosilicate

* Corresponding author at: Xinjiang Technical Institute of Physics & Chemistry, Chinese Academy of Sciences, 40-1 South Beijing road, Urumqi, Xinjiang 830011, China. Tel.: +86 911 3835879; fax: +86 911 3838957.
E-mail addresses: jiahz@ms.xjb.ac.cn (H. Jia), cywang@ms.xjb.ac.cn (C. Wang).

0926-3373/$ – see front matter © 2012 Elsevier B.V. All rights reserved.
http://dx.doi.org/10.1016/j.apcatb.2012.04.017

smectite clays as active components are especially important owing to their wide distribution in soils, high cation exchange capacity (CEC), large surface areas (~800 $m^2 g^{-1}$), and reversible interlayer expandability [17]. Thus, we hypothesize that smectite may play an important role on photolysis process of PAHs.

The principal objective of this study is to understand the photochemical behavior of phenanthrene at irradiated clay surfaces, attempting to (1) reveal the impact of clay type on photolysis, (2) probe the relative importance of the cation type and relevant speciation forms, and (3) further gain insight into the transformation pathway of PAHs and unveil the photolysis mechanisms. To the end, photolysis experiments were conducted on various types of clays following the protocol developed by Balmer and Schwarzenbach [11]. The protocol has proven to be feasible for studying photolysis of compounds sorbed onto dry, thin films of clay minerals with a controlled thickness [11,18].

2. Experimental

2.1. Chemicals and materials

Anhydrous ferric chloride ($FeCl_3$), sodium chloride (NaCl), calcium chloride ($CaCl_2$), cupric chloride ($CuCl_2$), sodium hydroxide (NaOH), hydrochloride acid (HCl, 36–38%), hydrofluoric acid (HF, 48%), perchloric acid ($HClO_4$, 70%), nitric acid (HNO_3, 68–70%) were obtained from Sinopharm Chemical Reagent Co., Ltd (Shanghai, China). Phenanthrene (Phe, 98%) and methanol (HPLC-grade solvent) were purchased from Sigma–Aldrich (Shanghai, China). All the chemicals were used as received. Kaolinite, vermiculite, and smectite clay minerals were obtained from Zhejiang Feng-Hong Clay Chemicals Co., Ltd (ZheJiang, China).

2.2. Preparation of phenanthrene contaminated clay

The preparation of Fe(III)-saturated clay minerals followed the method of Arroyo et al. [19]. Briefly, the clay suspension was first titrated to pH 6.8 with 0.5 M sodium acetate buffer (pH 5) to remove carbonate impurities. Clay-sized particles (<2 μm) were obtained by centrifugation of the clay suspension for 6 min at 600 rpm, and then treated with 0.1 M $FeCl_3$ solution for 4 times. The Fe(III)-saturated clay was washed using Milli-Q water until free of chloride as indicated by a negative test with $AgNO_3$. In order to prepare Fe(III)-smectite with different Fe(III) speciation forms, pH of involved suspension was adjusted to a desired value using 1.0 M HCl or NaOH, and then freeze-dried. Smectite clays saturated by other types of cations (e.g., Na^+, K^+, Ca^{2+}, Cu^{2+}) were achieved by following the same procedures described above except the substitution of 0.1 M Fe^{3+} by Na^+, K^+, Ca^{2+}, and Cu^{2+}. The clay samples before and after Fe(III) saturation were digested by the mixture of hydrofluoric acid, nitric acid and perchloric acid at 250 °C for 90 min, and Fe contents were determined using a PerkinElmer AAnalysis 400 Atomic Absorption Spectrophotometer (AAS, Norwalk, CT).

The reaction mixtures (phenanthrene contaminated clays) were prepared by mixing phenanthrene dissolved in 1 mL methanol with 1 g cation modified clays (0.1 mg phenanthrene/g clay) and the use of methanol allowed evaporating under ambient conditions.

2.3. Reaction of phenanthrene with cation-modified-clays under irradiation

The reaction was conducted at room temperature (23 °C) maintained inside a container consisting of two pieces of Quartz plates (9 cm × 9 cm × 2 mm), which were plated with a clay layer of controlled thickness using the method developed by Balmer and Schwarzenbach [11]. Briefly, contaminated clay was placed onto the center of the quartz glass plate. The area filled with the clay was controlled by a 2 mm thin Teflon gasket circular with an inner edge of 4 cm in diameter, resulting in a total surface area of 12.64 cm^2 to which the clay was applied. The thickness was determined from the mass and the bulk density of clay (e.g., 0.88 g/cm^3 for smectite). After that, the second quartz plate was placed on the Teflon gasket, and they were held together with binder clips. As-obtained clay plates were placed for irradiation under visible light of 0.250 W/cm^2 generated from a xenon lamp incorporated with an optical band-pass filter (the wavelength is in 380–780 nm). The distance between the lamp and samples was 100 mm. At pre-selected intervals, the samples were sacrificed and transferred into 50 mL Teflon centrifuge tubes. The residual phenanthrene and its products were extracted and analyzed immediately. For comparison, parallel experiments were conducted in dark as control.

2.4. Adsorption experiments

Various cation-modified clays (0.25 g) were placed into 15 mL glass centrifuge tubes and a 10 mL aliquot of phenanthrene solution of varying concentrations (0.025–1.0 mg L^{-1}) was added. Then the mixture was agitated using a shaker at 80 rpm in the dark at 23 ± 1 °C for 24 h. Kinetic measurements certified that 24 h was sufficient for the sorption of phenanthrene by all the minerals to attain equilibrium. After equilibration, the samples were taken and sacrificed for phenanthrene analysis in liquid phases.

2.5. Extraction and detection

Approximately 10 mL of extraction solution (mixture of 5 mL acetone and 5 mL dichloromethane) was added to each centrifuge tube containing specified clay samples. The suspensions were extracted in an ultrasonic bath for half an hour, and then centrifuged at 10,000 rpm for 10 min to separate the supernatants from the solids. The supernatants were collected and the solid residues were replenished with another 10 mL of extraction solution. Such procedure was repeated twice to assure all of the phenanthrene and its products were extracted. The supernatants were collected together, and filtered using a syringe filter equipped with a 0.22 μm membrane filter. The filtrates were stored in amber HPLC vials, and placed in a refrigerator prior to analysis.

Phenanthrene was quantified using a PerkinElmer HPLC equipped with a 25 cm × 4.6 mm Cosmosil C18 column. A 85:15 (v/v) mixture of methanol:water was employed as mobile effluent. The flow rate was 1.0 mL min^{-1}, and the ultraviolet detector was set at 254 nm. The phenanthrene and its intermediate products were identified using a PerkinElmer Packard gas chromatograph incorporated with a mass spectrometer operated on a full scan mode (35–500 amu), where a ZB-5 MS capillary column (length = 30 m; internal diameter = 250 μm; film thickness = 0.25 μm) was employed. Helium was used as carrier gas at a flow rate of 1.2 mL/min with splitless injection at 310 °C. The oven temperature was programmed from 60 °C to 220 °C (2 °C min^{-1}), and then to 300 °C (5 °C min^{-1}, 30 min hold).

3. Results and discussion

3.1. Effect by cations saturated in clays

In view of photo Fenton effect, it is hypothesized that the smectite clay saturated with transition metal ions would give higher reactivity compared to that saturated with other types of cations such as alkali metal ions. To test this hypothesis, the smectites saturated with different types of cations were prepared for photolysis experiments. The evolution of phenanthrene as a function of reaction time is presented in Fig. 1(a). After 6 h, approximately 100%, 64.8%, 29.5%, 24.7%, and 15.5% of initially added phenanthrene are transformed by photolysis associated with Fe^{3+}, Cu^{2+},

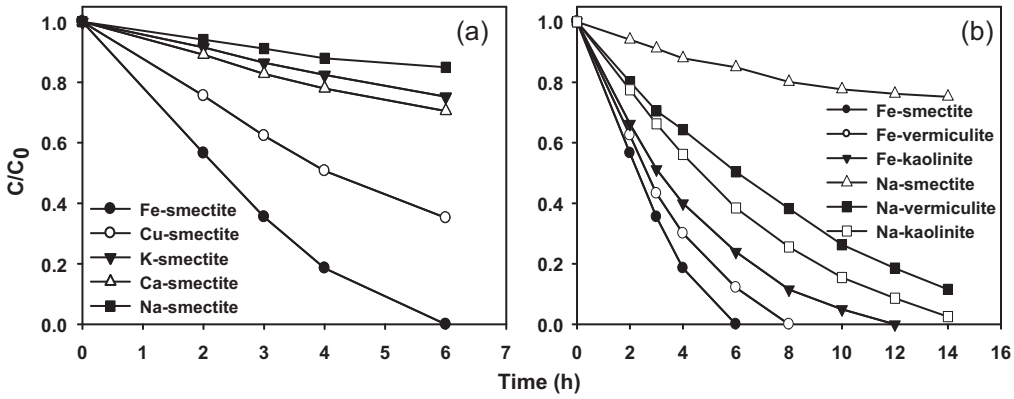

Fig. 1. The evolution of phenanthrene as a function of reaction time in the reaction system of (a) smectite modified by various cations; (b) smectite, vercumiculite, and kaolinite modified by Na^+ and Fe^{3+}, respectively.

Ca^{2+}, K^+ and Na^+ saturated smectite clays, respectively. Data fitting suggests that phenanthrene degradation follows a pseudo-first-order kinetic model in above stated reaction systems, and the plots of negative logarithmic normalized phenanthrene concentration versus reaction time are presented in Supporting Information (SI, Fig. 1(a)). It is concluded that the relevant photodegradation rate follows the order of Fe^{3+}-smectite > Cu^{2+}-smectite ≫ Ca^{2+}-smectite > K^+-smectite > Na^+-smectite. Insignificant disappearance of phenanthrene in dark control experiments suggests that its volatilization from the clay surface and dark reactions are negligible in the present reaction systems.

Fe(III)-containing minerals have been widely used in catalytic degradation of organic compounds [20]. For example, laponite loaded with Fe_2O_3 or intercalated with Fe(III) complex is a highly active catalyst for the photodegradation of Orange II under the irradiation of UV light (λ = 254 nm) [21]. The clay minerals modified by transition metal species (i.e., Fe(III) or Cu(II)) are also known as heterogeneous catalysts in the Fenton-like reactions [22]. In those studies, iron species play crucial roles in generating active sites and thus significantly enhance the reactivity of the mineral surface, which provides the necessary sites for Fe(III)/Fe(II) couple and stabilizes reactive radical cation intermediates [23,24]. Therefore, the phenanthrene degradation rate is greatly enhanced with exchangeable Fe^{3+} in the present study. Copper-containing Fenton-like system is much less active than the one containing iron for organic contaminant transformation [25], which is in agreement with what observed from the above stated reaction systems using clay minerals as catalysts. The significant differences between Fe-smectite (or Cu-smectite) and Na-smectite (or Ca-smectite) suggest that the degradation of phenanthrene is mainly due to the photo-Fenton-like reaction in the Fe-smectite system. However, opposite result was obtained in photodegradation of pesticides, which was enhanced in the presence of K^+-smectite compared with that of Fe(III) exchanged smectite [26].

In the absence of Fe^{3+} and Cu^{2+}, the Ca^{2+}-smectite exhibits greater photocatalytic activity than K^+-smectite and Na^+-smectite, which might be related to the adsorption capability of phenanthrene by cation modified clays. The phenanthrene adsorption experiments by different cation-modified smectites at room temperature were conducted and the adsorption isotherms are shown in Fig. 2. The adsorption isotherms give a good fit to the Freundlich model (r > 0.99). Ca^{2+}-modified smectite shows the highest adsorption capacity, followed by K^+-modified and then Na^+-modified, showing the same order as its reactivity for phenanthrene photodegradation. Hydrophobic interaction and interlayer accommodation are the dominant mechanisms of phenanthrene adsorption by clay minerals [5]. Due to strong hydration of Na^+, the local environment is surrounded with a large amount of water molecules, thus hinders the access of phenanthrene molecules to the siloxane sites to some extent and suppresses their adsorption. In the case of K^+-smectite, the weak hydration of K^+ makes it poor swelling, but the encumbrance of the solvated K^+ complex is far less than that of Na^+. As a result, the surface hydrophobicity of cation modified smectites follows the order of Na^+-modified < K^+-modified < Ca^{2+}-modified minerals, and the hydrophobicity order determines the capability of adsorbing hydrophobic phenanthrene onto the solid surfaces [27]. With the strong sorption of phenanthrene onto clays, the photochemistry of mineral surface-sorbed phenanthrene is of greater importance than photolysis of dissociative compounds. The transformation of phenanthrene is thereby very likely to occur on the clay surface during sorption. Therefore, Ca^{2+}-modified clay minerals generally show the highest catalytic activity, followed by K^+-modified and then Na^+-modified ones.

3.2. Effect of clay type

Iron contents in the original clays and Fe(III)-saturated clays are summarized in Table 1. The Fe content in the original clay samples originates mostly from structural iron, i.e., Fe exists in the layer structure due to isomorphic substitution. After saturating cation exchange sites with Fe^{3+}, the total Fe contents increase greatly, viz. 5.85% for smectite, 0.51% for kaolinite, and 4.62% for vermiculite. The exchangeable (vs. structural) Fe can be derived

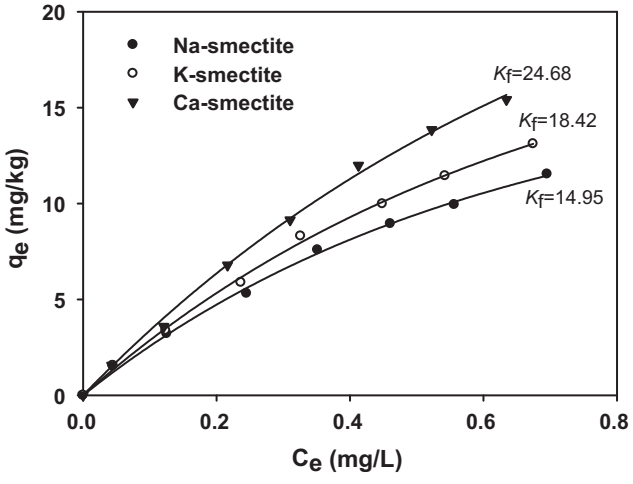

Fig. 2. Phenanthrene adsorption on the cation-modified smectite clay.

Table 1
Iron contents and relevant reaction rates of original and Fe(III)-saturated smectite, kaolinite, and vermiculite clays.

Clays	CEC (cmol(+) kg^{-1})	Na-saturated clay		Fe(III)-saturated clay	
		iron content (%)	pseudo-first-order rate constants k_{obs} (h^{-1})	iron content (%)	pseudo-first-order rate constants k_{obs} (h^{-1})
Smectite	82	2.80	0.0230	5.85	0.4094
Kaolinite	10	0.07	0.2039	0.51	0.2338
vermiculite	120	2.56	0.1508	4.62	0.3527

from the difference in iron contents between the original clays and the Fe(III)-saturated clays. The exchangeable iron contents were ca. 3.05%, 0.44%, and 2.06% for Fe(III)-saturated smectite, kaolinite and vermiculite, respectively. The content of Fe(III) species on clay surfaces is related to the structural negative charge density. With similar surface areas, mineral with greater surface charge density attracts greater density of exchangeable cations on the surfaces in principle. The structural negative charges of smectite are originated from isomorphic substitution, giving greater cation exchange capacity (CEC) than kaolinite, and the clay is expandable with accessible cation exchange sites presented in the interlayers as well as on the external surfaces of the stacked layer assemblages. Kaolinite has essentially no isomorphic substitution and the small amount of negative charges in these clays result mostly from the dissociation of hydroxides at edge sites, hence a small quantity of exchangeable Fe resides primarily on the external surfaces and edge sites. For vermiculite, though it possesses the greatest CEC, some of structural charges originating from isomorphic substitution are compensated by fixed K^+ which cannot be replaced by the added Fe^{3+} in the present work. Therefore, the exchangeable iron contents of clays studied here exhibit the order of smectite > vermiculite > kaolinite.

The loss of phenanthrene is quantified by the evolution of the molar ratio of phenanthrene concentration at a given time (C) to that at the beginning of the reaction (C_0) as a function of reaction time (Fig. 1(b)). It is noted that phenanthrene concentrations decrease gradually, and transformation of the phenanthrene associated with Fe^{3+}-smectite, Fe^{3+}-vermiculite, and Fe^{3+}-kaolinite clays could be completed in approximately 6, 8 and 14 h, respectively. Kinetic studies find that phenanthrene degradation observes a pseudo-first-order reaction model in the three studied clay systems (SI, Fig. 1(b)) and the pseudo-first-order rate constants (k_{obs}) are listed in Table 1. As a result, phenanthrene photodegradation rate follows the order of Fe^{3+}-smectite > Fe^{3+}-vermiculite > Fe^{3+}-kaolinite, which is in agreement with the exchangeable iron contents presented in the clays. The oxidative capability of Fe-clay to degrade phenanthrene may be correlated to the cation exchange capacity of the clay layered structures, which determines the Fe(III) populations that serve as electron acceptor sites. Fe(III) species on smectite and vermiculite surfaces are more enriched leading to a higher reactivity of phenanthrene photolysis. Compared to smectite and vermiculite, kaolinite provides less active sites as indicated by the number of Fe(III) species adsorbed on the clay surface, and thereby it gives smaller rate of phenanthrene degradation. To investigate the effect by the other intrinsic properties of different clays on phenanthrene transformation, the photodegradation experiments were systematically conducted using three types of Fe^{3+}-modified clays including smectite, vermiculite, and kaolinite with controlled amount of Fe content (~0.45 wt% to clay). Consequently, comparable rates were observed for phenanthrene degradation in the three studied clay systems (for details, refer SI Fig. 2). This supports what fore-stated, i.e., the phenanthrene photodegradation is mainly correlated to the exchangeable iron content on Fe-saturated clays. This result is in agreement with the Fenton-like system using Fe pillared clays as catalysts, in which the contaminant conversion rate is directly related to the iron contents [25].

For the clays saturated by Na^+, phenanthrene photodegradation rate follows the order of smectite < vermiculite < kaolinite, which is inversed with what observed for the clays associated with Fe^{3+} (Table 1). Na^+-smectite with a large content of structural iron shows limited photocatalytic activity, suggesting that structural iron plays an insignificant role in phenanthrene degradation in this case. However, the phenanthrene degradation rate at Na-kaolinite is one-order of magnitude higher than at Na-smectite (SI, Fig. 1(b)). This can be attributed to the difference in adsorption properties brought by various clays. The basal planes of the low-charged clays (i.e., kaolinite) are expected to be less hydrated than those of the high-charged clays (i.e., smectite) because fewer hydrated cations are attracted to them, making the uncharged siloxane surfaces relatively hydrophobic [28]. Thus, kaolinite has greater sorption affinity and degradation rate for phenanthrene [29]. Clay minerals such as smectite with high exchange capacities and swelling properties affect phenanthrene sorption/retention and thus photochemical behavior. In the absence of Fenton agents such as Fe^{3+} or Cu^{2+}, photolysis rate is likely to be determined by the interaction of phenanthrene with mineral surfaces.

3.3. Effect of water content in Fe(III)-smectite

As mentioned above, the hydration status of cations adsorbed on clay surface could influence the adsorption and photodegradation of phenanthrene. In the present study, the reactivity of various Fe(III)-smectite samples with different water contents was evaluated by following the process of phenanthrene photodegradation. Kinetic studies find that phenanthrene degradation observes a pseudo-first-order reaction model in Fe(III)-smectite systems with different water contents. The pseudo-first-order rate constants (k_{obs}) as a function of water contents are presented in Fig. 3. The reaction rate constant increases significantly from 0.462 to 0.522 h^{-1} when the water content increases from 0% to 5%. After the water content is beyond 10%, the reaction rate constant is little changed. The increase in photodegradation rate with the presence

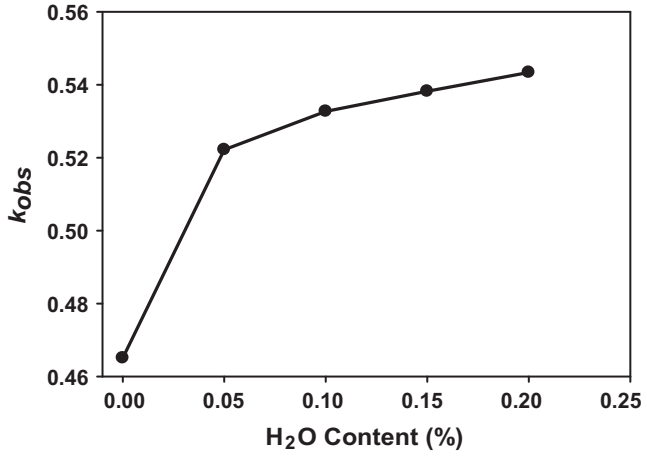

Fig. 3. Effect of water content on phenanthrene degradation with Fe(III)-smectite.

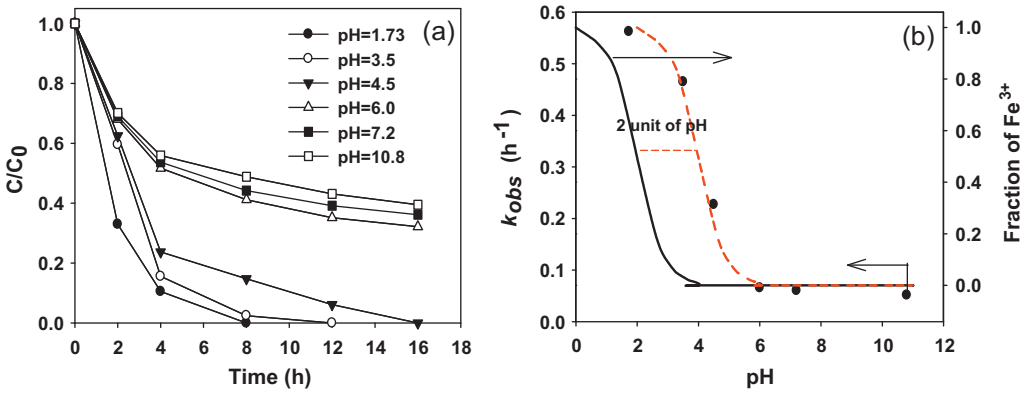

Fig. 4. (a) photodegradation of phenanthrene by Fe(III)-smectite prepared at various pHs, (b) The evolution of the pseudo-first-order rate constant for phenanthrene degradation as a function of pH value.

of a certain amount of water is understandable because of the following. Firstly, photo-Fenton-like reaction involves intermediate species such as superoxide radical anions ($O_2^{\bullet -}$) and holes; they can react with water (H_2O) to produce hydroxyl radicals ($OH^{\bullet}$) which are highly oxidative species and can enhance the degradation of phenanthrene adsorbed on clay surfaces. Secondly, there is a direct radiation effect; water greatly increases the amount of radiation absorbed in the soil [10]. However, higher water content could induce greater extent of hydration, and a large amount of water molecules surrounding with Fe(III) will hinder the access of the phenanthrene molecules to the siloxane sites, thus inhibiting the revelvant photochemical behavior. Therefore, photodegradation rate cannot further increase linearly with increasing water content in Fe(III)-smectite.

Water content and exchangeable cation type of clay minerals are considered as important factors that affect the cation hydration, and thus PAHs adsorption to mineral surfaces [30]. The observed water effect on the photodegradation of phenanthrene in Fe(III)-smectite is different from what in Na-smectite, which could be understood as follows. For dehydrated Na-saturated smectite clay, phenanthrene is adsorbed on the clay surface through Na^+—π bonding. Upon water addition, the readily hydration of Na^+ induces coverage with water molecules on smectite surface, which leads to a rapid detachment of phenanthrene from the mineral surface. Therefore, the hydration of cation could hinder the access (adsorption) of the phenanthrene to cation and/or mineral surface, thus inhibiting the revelvant photochemical behavior. However, iron as a transition metal can interact with aromatic rings of organic compounds (such as phenanthrene), which results in higher adsorption and stronger inner-sphere complexation on the Fe^{3+}-smectite clay surface [30–32]. The restrained effect of cation hydration on retention of phenanthrene on Fe^{3+}-smectite surface is expected compared to Na^+-smectite, and a small amount of water accelerates the photodegradation.

3.4. Effect of pH and Fe species

Depending on pH, the Fe(III) species exist in various hydrate states in aqueous environment. Therefore, the reactivity assisted by Fe(III) species varies with pH-related local chemical microenvironments [33]. In the present study, the reactivity of various Fe(III)-smectite samples prepared under different pH conditions was evaluated by phenanthrene photodegradation. The phenanthrene remediation results associated with various Fe(III)-smectite samples are supplied in Fig. 4(a). As a trend, photodegradation rate decreases with increasing pH over the range of 1.7–10.8. When pH value is 1.7, almost 90% of phenanthrene is degraded in 4 h. As pH is adjusted to 4.5 and 6.0, nearly 23.7% and 51.7% of phenanthrene remains as residues in 4 h of photodegradation, respectively (Fig. 4 (a)). Further increasing pH to 7.2 and 10.8, similar degradation rate is obtained as that for pH 6.0. Kinetic studies suggest that phenanthrene degradation follows a pseudo-first-order reaction model and the rate constants (k_{obs}) for phenanthrene degradation as a function of pH are shown in SI Fig. 3. The k_{obs} value is 0.56 h^{-1} when pH is 1.7, but it decreases rapidly with increasing of pH value in the range of 1.7–6.0, and then is nearly kept as constant when pH is further increased up to 10.8. When pH is ~6, the degradation rate is 0.065 h^{-1}, which is about one order of magnitude less than that at pH 1.7.

Previous studies have established that the species of iron associated with cation exchangeable sites in smectite clays are strongly dependent on pH [34,35]. In this context, both the photodegradation rate constant of phenanthrene (k_{obs}) and the fractions of Fe^{3+} are correlated against pH (Fig. 4(b)). It is noted that the k_{obs} value decreases in parallel to the trend of Fe(III) fraction change as a function of pH. Shifting the Fe(III) fraction change curve along the X-axis for 2 pH units, the k_{obs} value in the range of pH 1.7–10.8 is coincident with the change in the Fe^{3+} fractions. This can be explained by the fact that interlayer pH is approximate 2 units lower than that of the bulk solution due to the existence of both Lewis and Brønsted acidity sites on the Fe-smectite surface [36–39]. When pH is >2, Fe(III) compensating the negative charges exists as mixed hydroxide complexes in the form of $[Fe(OH)_{1-4}]_n^{-1-2+}$ and amorphous iron oxyhydroxides, rather than simple Fe^{3+} ions [34,35]. Under acidic condition (i.e., pH < 2), precipitation or hydroxylation of Fe(III) is unlikely to occur. Therefore, the hydroxyl iron polymers are readily depolymerize and Fe(III) is then released after the suspension is adjusted to ~2 rather than zero [40]. This observation implies Fe^{3+} as the predominant species for activating photodegradation. Therefore, the decrease in the degradation rate of phenanthrene with increasing pH is presumably resulted from reducing Fe^{3+} fraction.

It is well known that typical Fenton reaction ($Fe^{2+} + H_2O_2$) generally occurs at the acidic conditions, thus iron precipitation is avoided. On the other hand, heterogeneous solid catalysts can mediate Fenton-like reaction over a wide range of pH values [20,41]. Being strongly bound to exchangeable sites within the pore/interlayer structure, transition metals (e.g., iron and copper) are not prone to leach out or precipitate during the process [42]. In other words, iron hydroxide precipitation is prevented over a wide pH range in the system of Fe(III)-smectite, and the catalyst can maintain its capability to generate hydroxyl radicals or other oxidant during photo Fenton-like processes. Notice that Fe^{3+} is the only species being able to absorb light appreciably in the visible region leading to photolysis in the present study, which is in agreement with other reports [43]. Besides, the Fe(III)-smectite prepared here contains very small amount of associated Fe-oxide phase (beyond

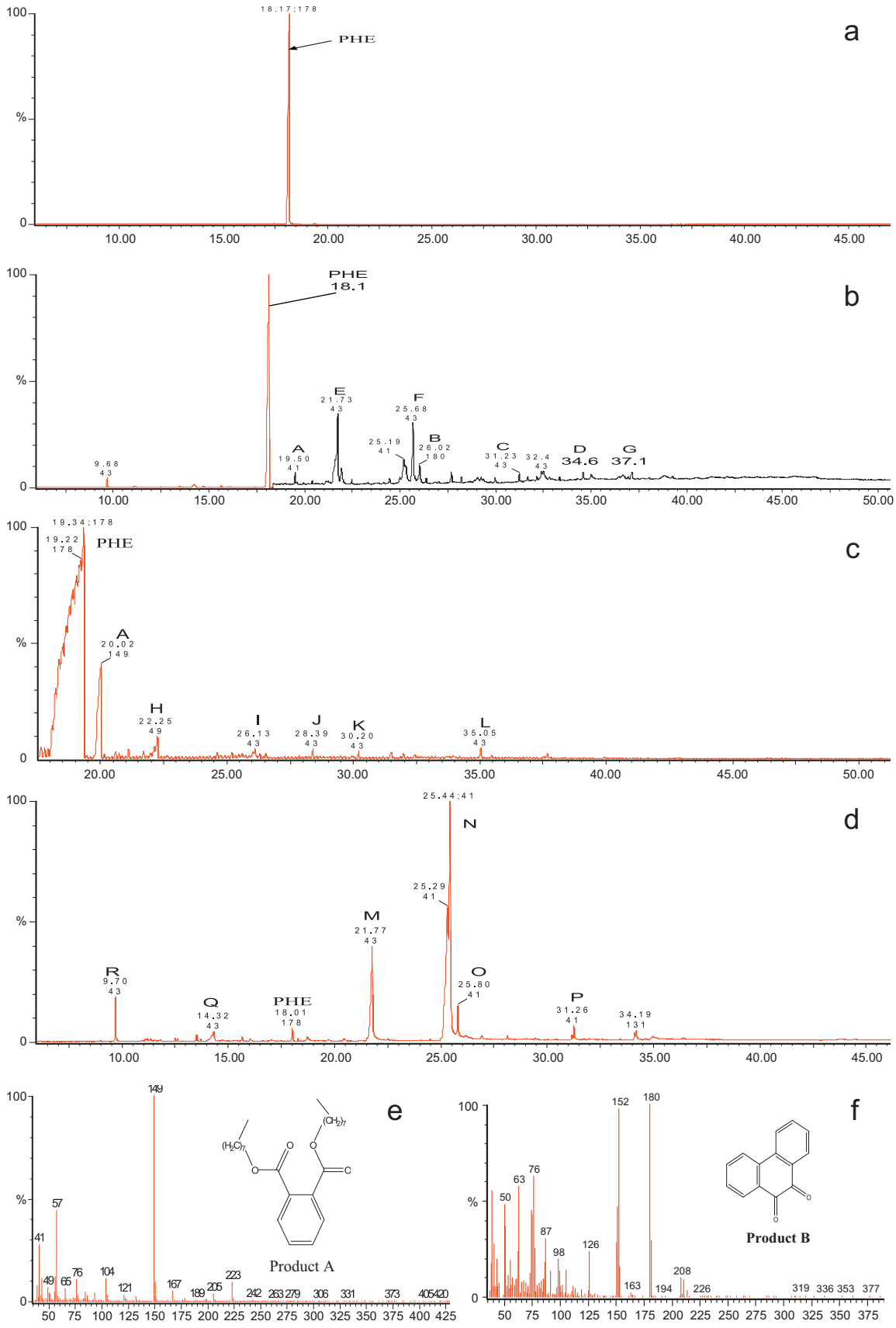

Fig. 5. GC–MS chromatograms of extracting of the Fe(III)-montmorillonite/phenanthrene photolysis reaction mixture after (a) 0 h, (b) 2 h, (c) 4 h and (d) 6 h reaction time. Mass spectra of relevant products: (e) product A (retention time of 19.9 min), and (f) product B (retention time of 21.9 min).

Table 2
Identification of intermediates produced during degradation of phenanthrene based on GC–MS measurements.

Peak	Reaction time	Retention time	*m/z*	Empirical formula	Product
C		31.23	256	$C_{16}H_{32}O_2$	pentadecanoic acid methyl ester
D		34.6	270	$C_{17}H_{34}O_2$	heptadecanoic acid methyl ester
E	2 h	21.73	256	$C_{16}H_{32}O_2$	hexadecanoic acid
F		25.68	284	$C_{18}H_{36}O_2$	octadecanoic acid
G		37.1	238	$C_{15}H_{26}O$	3,7,11-trimethyl-2,6,10-dodecatrien-1-ol
H		22.25	256	$C_{16}H_{32}O_2$	hexadecanoic acid
I		26.13	280	$C_{18}H_{32}O_2$	octadecanoic acid
J	4 h	28.39	240	$C_{17}H_{36}$	2,4,6-trimethyl-tetradecane
K		30.2	158	$C_{10}H_{22}O$	2-propyl-heptan-1-ol
L		35.05	156	$C_{11}H_{24}$	3-ethyl-nonane
M		21.77	240	$C_{15}H_{28}O_2$	pentadecanoic acid
N		25.44	256	$C_{16}H_{32}O_2$	hexadecanoic acid
O	6 h	25.80	284	$C_{18}H_{36}O_2$	octadecanoic acid
P		31.26	298	$C_{18}H_{34}O_3$	2-acetyl-tetradecanoic acid ethyl ester
Q		9.7	130	$C_7H_{14}O_2$	2-ethyl-5methyl-[1,4]dioxane
R		14.32	176	$C_8H_{16}O_3$	1-(2,2-dimethy-[1,3]dioxan-4-yl)-ethanol

detection limit here by the conventional techniques such as XRD, IR etc.), the phenanthrene remediation is unlikely to be attributed to the semiconductor photocatalysis induced by iron oxides.

3.5. Transformation pathway

The photodegradation of phenanthrene was conducted by Fe(III)-smectite prepared under pH 3.5. At pre-selected reaction intervals (i.e., 2 h, 4 h and 6 h), the samples were sacrificed and major products were obtained by extraction of the clay with 1:1 acetone/dichloromethane. These products were identified by GC–MS analysis. Fig. 5 displays the GC–MS chromatograms of phenanthrene photodegradation after 2 h, 4 h, and 6 h of visible light irradiation and the corresponding mass spectra related to GC peaks A, and B. The characteristics of other main peaks are shown in Table 2. It is noted that peak B gives the maximum *m/z* value of 208, among the intermediates of the photodegradation of phenanthrene. According to the standard spectra from the NIST library database, the peak of B can be assigned to 9,10-Phenanthrenequinone. Correspondingly, the peak A (shown a retention time of 19.5) can be tentatively assigned to compound of phthalate by analyzing the fragmentation pattern of mass spectra, which was not be observed in control sample (Fig. 5a). Based on the results of GC–MS spectral analysis, minor portions of phthalates, and 9,10-phenanthrenequinone (denoted as product A, and B) were detected during 2 h of irradiation. Product B, formed by ketonizing the intermediate benzene ring of phenanthrene, is considered as a major photodegradation intermediate as previously reported [44]. However, this product can no longer be found in the samples of 4 h and 6 h irradiation in the present study. On the other hand, the concentration of product A significantly increases as the reaction proceeds and becomes a major product when the sample was irradiated for 4 h. This suggests the potential accumulation of phthalate, which is one kind of the plasticizer used in industry and is considered as hazardous material to human health. This is in agreement with the observation previously report, in which phthalates were detected as the main intermediates of phenanthrene photodegradation by TiO_2 under UV irradiation [45].

Other remaining major products, such as intermediates for peaks C, D, and P are identified as esters, E, F, H, I, O, N and M are identified as alkanoic acids, G and K are alkanols, J and L are identified as alkanes, Q and R are dioxanes respectively (Table 2). Most of those products can be found in the 2 h irradiated samples. After 6 h of reaction, insignificant portion of phenanthrene remains and the residual products are alkanoic acids and esters, indicating the photodegradation of phenanthrene by Fe(III)-smectite. The results are also in agreement with what previously studied, in which products such as ring-opened aldehyde, phthalic derivatives, and alkane/alkene are identified as main intermediates in the process of Benzo[*a*]pyrene oxidation by O_3/$^{\bullet}$OH [46]. And the aldehyde and acid were abundant at the initial stage, while the alkene and alkane were more prevalent in the later stage, which agrees well with the present observation. In addition, no significant products can be detected for the reactions with ferric salts, or in the absence of Fe-smectite, and only minor yields of products (<5%) are obtained with homoionic Na-smectite or Ca-smectite compared to that of the Fe(III)-smectite.

Note that the above stated intermediates represent only portion of the reaction intermediates, since some intermediates had very short lifetimes and could not be detected in the current GC–MS analysis. The degradation pathways are tentatively proposed as in Fig. 6. In the photo-Fenton-like reaction system, hydroxyl radicals and singlet oxygen are considered as the major oxidizing species, which can preferentially attack phenanthrene at positions 9 and 10 to yield theoretical products 1–2 [47]. Further oxidation leads to substituted products such as 9,10-Phenanthrenequinone, which has been detected as one of the main products in previous reports [45,47,48]. Intermediate 9,10-Phenanthrenequinone could be cleaved to yield product 3 with subsequent destruction to produce phthalate (product 4) [49,50]. The formed phthalate could be esterified into diisobutyl phthalate in OH-induced oxidation process [45,51]. After further cleavage over the rest benzene ring, various alkanes, such as esters, alkanoic acids, alkanols, alkanes, dioxanes, are formed [52,53]. Given sufficient reaction time, all the intermediates could be completely mineralized.

3.6. Mechanism of phenanthrene photodegradation on Fe(III)-smectite surface

Photo-Fenton reaction has been considered as one of the most appropriate AOP (advanced oxidation processes) techniques for removal of organic toxicants because it may occur naturally. Fe(III)-smectite exhibits notable absorption under visible-light (as shown in SI Fig. 4) and could act as natural photocatalyst to catalyze degradation of organic pollutants in environment [20]. In the present study, Fe(III)-smectite is irradiated and transforms into Fe(II)-smectite after receiving electrons (Eq. (1)), and the oxidation process may proceed by one electron transfer leading to the formation of the phenanthrene radical cations [53]. The strong adsorption of phenanthrene on the clay layers facilitates the electron transfer from the exited Fe(III)-smectite to organic molecules and such transfer can initiate the photodegradation of

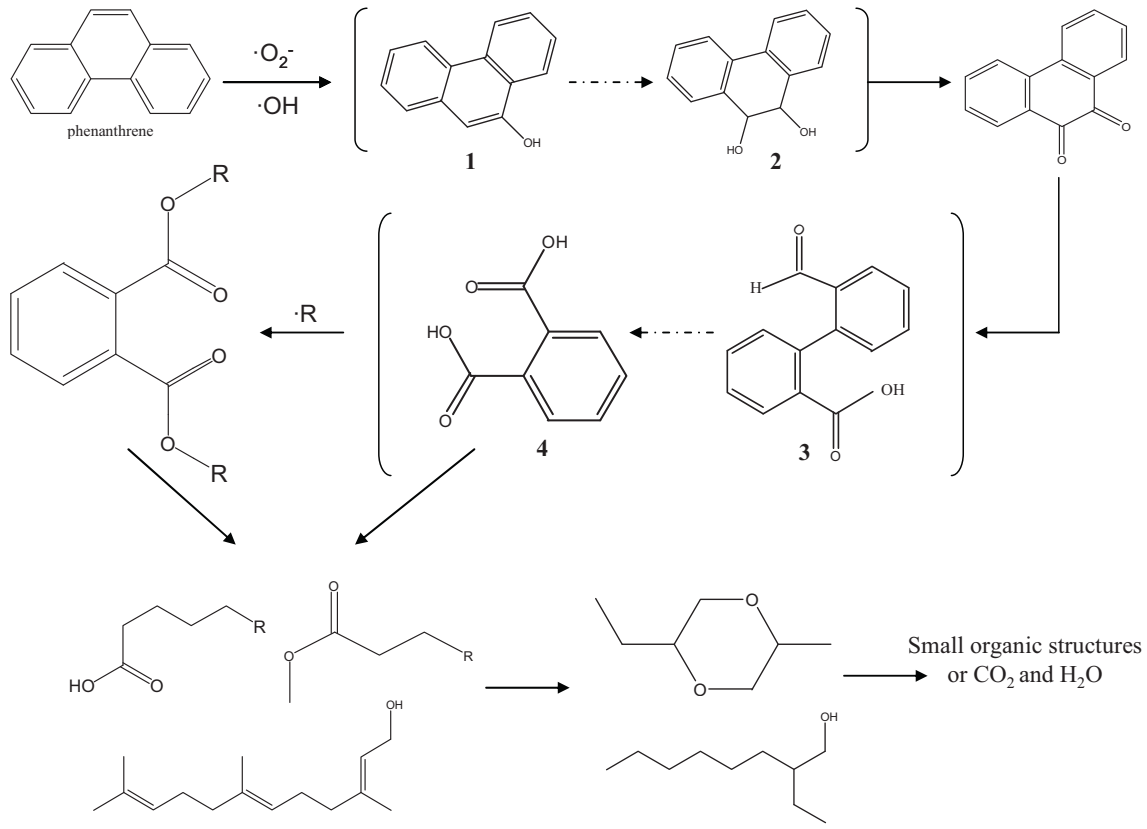

Fig. 6. Proposed mechanism for the photodegradation of phenanthrene with Fe(III)-smectite.

phenanthrnene. Meanwhile, hydroxyl radicals (•OH) with high redox potential are generated after the capture of h^+ from Phe^+ by water molecules (Eq. (2)) [53]. The transient smectite-Fe(II) is reoxidized to smectite-Fe(III) with concomitant formation of superoxide radicals such as O_2^- and HO_2• in the presence of O_2 (Eqs. (3) and (4)) [54,55]. The formed O_2•$^-$/HO_2• then is transformed into H_2O_2 by disproprotionation (Eq. (5)). Accordingly, the system containing Fe(II) and H_2O_2 is able to perform a Fenton-like reaction to generate •OH (Eq. (6)) [55]. And then PAHs could be oxidized and further mineralized by •OH and O_2^- (Eq. (7)) [56,57].

$$\text{Fe(III)-smectite-PHE} \xrightarrow{h\nu} \text{Fe(II)-smectite-PHE}^+(\text{visible light}) \quad (1)$$

$$H_2O + Phe^+ \rightarrow H^+ + {}^\bullet OH \quad (2)$$

$$\text{Fe(II)-smectite} + O_2 \rightarrow \text{Fe(III)-smectite} + O_2^- \quad (3)$$

$$O_2^- + H_2O \rightarrow HO_2^\bullet \quad (4)$$

$$2HO_2^\bullet + \text{Fe(II)-smectite} \rightarrow H_2O_2 + O_2 + \text{Fe(III)-smectite} \quad (5)$$

$$\text{Fe(II)-smectite} + H_2O_2 \rightarrow \text{Fe(III)-smectite} + {}^\bullet OH + OH^- \quad (6)$$

$$\text{PAHs} + {}^\bullet OH(\text{or}\ {}^\bullet O_2^-) \rightarrow \text{degradationproducts} \quad (7)$$

The degradation of phenanthrene on clay mineral under irradiation is mainly due to photo-oxidation, which is enhanced Fenton-like oxidative degradation in the presence of Fe^{3+}. However, in the absence of transition metal ions (such as Na^+-smectite or Ca^{2+}-smectite), the photochemical oxidation is proposed to involve an electron transfer from the excited singlet state of phenanthrene to molecule oxygen directly to form singlet oxygen, which readily reacts with another molecule of phenanthrene to give endoperoxide and continued irradiation of phenanthrene and endoperoxide ultimately leads to diones (quinones) and other products [58,59].

4. Conclusions

Fe(III)-saturated smectite clay exhibits great activity to catalytic photodegradation of phenanthrene, indicating that the photochemistry of phenanthrene is of great importance in the soil environment. The transformation of phenanthrene via photodegradation on clay surface provides valuable insights on the fates of phenanthrene in the natural soil environment. The present study also opens up a window of using natural catalysts for the treatment of industrial contaminants. Due to their compelling merits for effective removal of organic pollutants in soil and sediment together with great abundance in nature, the clays (e.g., cation-modified smectite) have great potential to act as catalysts for the practical treatment of PAHs in soil on a large scale. From the point of economic and practical view, cation-modified clay minerals as catalysts for photo-Fenton-like reactions hold great promise in the remediation of contaminated soil, sediment, and industrial fields.

Acknowledgements

Financial support by the National Natural Science Foundation of China (21173261), the "One Hundred Talents" program of Chinese Academy of Sciences (1029471301), the International Cooperation Program of Xinjiang Uygur Autonomous Region (20126017) and the "Western Light" program of Chinese Academy of Sciences (XBBS201112) is gratefully acknowledged.

Appendix A. Supplementary data

Supplementary data associated with this article can be found, in the online version, at http://dx.doi.org/10.1016/j.apcatb.2012.04.017.

References

[1] X.J. Li, X. Lin, C.G. Zhang, Q. Li, Z.Q. Gong, Journal of Hazardous Materials 150 (2008) 21.
[2] L. Albert, R.N. Juhasz, International Biodeterioration & Biodegradation 45 (2000) 57.
[3] K.S. Samanta, O.V. Singh, R.K. Jain, Trends in Biotechnology 20 (2002) 243.
[4] N.M. Price, M.R. Landry, F.K. Azam, J.F. Hall, Marine Ecology Progress Series 34 (1986) 41.
[5] L.C. Zhang, L.L. Shu, Z. Zhang, Colloids and Surfaces A: Physicochemical and Engineering Aspects 377 (2011) 278.
[6] F. Richard, W.S. Lee, J.W.G. Anderson, J.W. Blaylock, J. Barwell-Clarke, Environmental Science and Technology 12 (1978) 832.
[7] L.H. Zhang, C.X. Zhong, L. Chen, X. Li, P.J. Li, Journal of Hazardous Materials 173 (2010) 168.
[8] Y. Wang, C.S. Liu, F.B. Li, C.P. Liu, J.B. Liang, Journal of Hazardous Materials 162 (2009) 716.
[9] L.H. Zhang, Z.Q. Gong, A.A. Oni, Journal of Environmental Sciences 18 (2006) 1226.
[10] D.B. Dong, X.J. Li, C.B. Xu, D.W. Gong, Y.Q. Zhang, Q. Zhao, P. Li, Chemical Engineering Journal 158 (2010) 378.
[11] E.M. Balmer, P.R. Schwarzenbach, Environmental Science and Technology 34 (2000) 1240.
[12] I. Cavoski, P. Caboni, G. Sarais, P. Cabras, T. Miano, Journal of Agricultural and Food Chemistry 55 (2007) 7069.
[13] X.Z. Fan, B. Lu, A.J. Gong, Journal of Hazardous Materials 117 (2005) 75.
[14] S.W. Chang Chien, C.H. Chang, S.H. Chen, M.C. Wang, M.M. Rao, S.S. Venia, Science of The Total Environment 409 (2011) 4078.
[15] B.L. Chen, W.H. Huang, J.F. Mao, S.F. Lv, Journal of Hazardous Materials 158 (2008) 116.
[16] H. Li, G.Y. Sheng, B.J. Teppen, C.T. Johnston, S.A. Boyd, Soil Science Society of America Journal 67 (2003) 122.
[17] B.L. Allen, B.F. Hajek, W.I. Madison, Soil Science Society of America Journal (1989) 199.
[18] A. Ciani, K.U. Goss, P.R. Schwarzenbach, Environmental Science and Technology 39 (2005) 6712.
[19] L.J. Arroyo, H. Li, J.B. Teppen, A.S. Boyd, Clays and Clay Minerals 53 (5) (2005) 511.
[20] M.M. Cheng, W. Song, W.H. Ma, C.C. Chen, J.C. Zhao, J. Lin, H.Y. Zhu, Applied Catalysis B: Environmental 77 (3–4) (2008) 355.
[21] M.M. Cheng, W. Ma, C.C. Chen, J.N. Yao, J.C. Zhao, Applied Catalysis B: Environmental 65 (3–4) (2006) 217.
[22] P. Ciésla, P. Kocot, P. Mytych, Z. Stasicka, Journal of Molecular Catalysis A: Chemical 224 (2004) 17.
[23] C. Gu, H. Li, B.J. Teppen, S.A. Boyd, Environmental Science and Technology 42 (2008) 4758.
[24] S.A. Boyd, M.M. Mortland, Environmental Science and Technology 20 (1986) 1056.
[25] J. Barrault, J.M. Tatibouët, N. Papayannakos, Surface Chemistry and Catalysis 3 (10) (2000) 777.
[26] L. Tajeddinea, H. Mountacera, M. Sarrakha, Arabian Journal of Chemistry 3 (2) (2010) 73.
[27] L. Luo, S. Zhang, Y.B. Ma, P. Christie, H.L. Huang, Environmental Science and Technology 42 (7) (2008) 2414.
[28] D.A. Laird, Clays and Clay Minerals 47 (5) (1999) 630.
[29] J. Jeffrey, K.M. Werner, A.W. Arnold, Journal of Agricultural and Food Chemistry 57 (15) (2009) 6932.
[30] D. Zhu, B.E. Herbert, M.A. Schlautman, E.R. Carraway, J. Hur, Journal of Environment Quality 33 (2004) 1322.
[31] K.H. Kung, M.B. McBride, Soil Science Society of America Journal 53 (1989) 1673.
[32] T. Polubesova, Y. Chen, R. Navon, B. Chefetz, Environmental Science and Technology 42 (2008) 4797.
[33] K. Pecher, S.B. Haderlein, R.P. Schwarzenbach, Environmental Science and Technology 36 (8) (2002) 1734.
[34] M.S. Tzou, Ph.D. Dissertation, Michigan State University, East Lansing, MI (1983).
[35] J. Manjanna, T. Kozakki, S. Sato, Applied Clay Science 43 (2009) 208.
[36] M.M. Mortland, Advances in Agronomy 22 (1970) 75.
[37] G.W. Bailey, J.L. White, T. Rothberg, Soil Science Society of America Journal 32 (1968) 222.
[38] M.M. El-amamy, T. Mill, Clays and Clay Minerals 32 (1) (1984) 67.
[39] G.W. Bailey, D.S. Brown, S.W. Karickhoff, Science 182 (4114) (1973) 819.
[40] C. Gu, H.Z. Jia, H. Li, J.B. Teppen, A.S. Boyd, Environmental Science and Technology 44 (11) (2010) 4258.
[41] S. Caudoa, G. Centia, C. Genovesea, S. Perathoner, Applied Catalysis B: Environmental 70 (1–4) (2007) 437.
[42] M. Neamtu, C. Zaharia, C. Catrinescu, A. Yediler, M. Macoveanu, A. Kettrup, Applied Catalysis B: Environmental 48 (4) (2004) 287.
[43] M.M. Cheng, W. Ma, J. Li, Y.P. Huang, J.C. Zhao, Environmental Science and Technology 38 (5) (2004) 1569.
[44] B.D. Boule, P. Boule, Chemosphere 26 (9) (1993) 1617.
[45] Y.L. Zhang, J.W.C. Wong, P.H. Liu, M. Yuan, Journal of Hazardous Materials 191 (2011) 136.
[46] Y. Zeng, P.K. Hong, A.D. Wavrek, Environmental Science and Technology 34 (2000) 854.
[47] O.T. Woo, W.K. Chung, K.H. Wong, T.A. Chow, P.K. Wong, Journal of Hazardous Materials 168 (2009) 1192.
[48] J.R. Odum, S.R. Mcdow, R.M. Kamens, International Symposium Measurement of Toxic and Related Air Pollutants, May 4-7, Durham, North Carolina, USA, 1993.
[49] H. Kang, S.Y. Hwang, Y.M. Kim, E. Kim, Y.S. Kim, S.K. Kim, S.W. Kim, C.E. Cerniglia, K.L. Shuttleworth, G.J. Zylstra, Canadian Journal of Microbiology 49 (2003) 139.
[50] J.H. Kou, Z.S. Li, Y.P. Yuan, H.T. Zhang, Y. Wang, Z.G. Zou, Environmental Science and Technology 43 (2009) 2919.
[51] T. Cajthaml, P. Erbanova, V. Sasek, M. Moeder, Chemosphere 64 (2006) 560.
[52] T. Mill, W.R. Mabey, B.Y. Lan, A. Baraze, Chemosphere 10 (11–12) (1981) 1281.
[53] S.J. Miller, D. Olejnik, Water Research 35 (1) (2001) 233.
[54] J. Sýkora, Coordination Chemistry Reviews 159 (1997) 95.
[55] C.L. Yap, S. Gan, H.K. Ng, Chemosphere 83 (2011) 1414.
[56] J. Sykora, Coordination Chemistry Reviews 159 (1997) 95.
[57] S. Konrad, M. Wojciech, D.M. Agnieszka, B. Magorzata, Y.S. Graz, Chemical Reviews 105 (2005) 2647.
[58] M.A. Fox, S. Olive, Science 205 (4406) (1979) 582.
[59] B. Rånby, J.F. Rabek, Photodegradation, Photo-oxidation, and Photostabilization of Polymers Principles and Applications, John Wiley & Sons Ltd, 1975.